Thermal Dissociation of SO_3 at 1000−1400 K†

Ayten Yilmaz, Lusi Hindiyarti, Anker D. Jensen, and Peter Glarborg*

Department of Chemical Engineering, Technical University of Denmark, DK-2800 Lyngby, Denmark

Paul Marshall

Department of Chemistry, University of North Texas, P.O. Box 305070, Denton, Texas 76203-5070

Received: October 7, 2005; In Final Form: December 15, 2005

The thermal dissociation of SO_3 has been studied for the first time in the 1000−1400 K range. The experiments were conducted in a laminar flow reactor at atmospheric pressure, with nitrogen as the bath gas. On the basis of the flow reactor data, a rate constant for $SO_3 + N_2 \rightarrow SO_2 + O + N_2$ (R1b) of $5.7 \times 10^{17} \exp(-40000/T)$ $cm^3/(mol\ s)$ is derived for the temperature range 1273−1348 K. The estimated uncertainty is a factor of 2. The rate constant corresponds to a value of the reverse reaction of $k_1 \approx 1.8 \times 10^{15}$ $cm^6\ mol^{-2}\ s^{-1}$. The reaction is in the falloff region under the investigated conditions. The temperature and pressure dependence of $SO_2 + O\ (+N_2)$ was estimated from the extrapolation of low temperature results for the reaction, together with an estimated broadening parameter and the high-pressure limit determined recently by Naidoo, Goumri, and Marshall (*Proc. Combust. Inst.* **2005**, *30*, 1219−1225). The theoretical rate constant is in good agreement with the experimental results. The improved accuracy in k_1 allows a reassessment of the rate constant for $SO_3 + O \rightarrow SO_2 + O_2$ (R2) based on the data of Smith, Tseregounis, and Wang (*Int. J. Chem. Kinet.* **1982**, *14*, 679−697), who conducted experiments on a low-pressure $CO/O_2/Ar$ flame doped with SO_2. At the location in the flame where the net SO_3 formation rate is zero, $k_2 = k_1[SO_2][M]/[SO_3]$. A value of 6.9×10^{10} $cm^3\ mol^{-1}\ s^{-1}$ is obtained for k_2 at 1269 K with an uncertainty a factor of 3. A recommended rate constant $k_2 = 7.8 \times 10^{11} \exp(-3065/T)$ $cm^3\ mol^{-1}\ s^{-1}$ is consistent with other flame results as well as the present flow reactor data.

Introduction

Research in high-temperature sulfur chemistry has been motivated partly by the effect of sulfur species on flame characteristics and nitrogen chemistry and partly by the adverse effects of a high SO_3/SO_2 ratio in the flue gas. During the combustion of sulfur-containing fuels, most of the sulfur is converted to sulfur dioxide (SO_2) but a small fraction is oxidized further to form sulfur trioxide (SO_3). The presence of SO_3 enhances the corrosion potential of the flue gas,[1] and it has implications for the formation of aerosols in biomass-fired systems.[2−4]

The conversion of SO_2 to SO_3 is kinetically limited[1]. The reactions that may contribute to the formation of SO_3 involve the interaction of SO_2 with the radical pool.[5−7] In the presence of nitrogen oxides, there is a kinetic coupling of NO_x and SO_x chemistry via the radical pool.[5,7] While the overall mechanisms for SO_3 formation are fairly well-known, kinetic modeling of the process still suffers from a lack of accurate kinetic data and refinements are required in order to establish a reliable mechanism.[4,5]

Flow reactor studies of SO_2 oxidation under post-flame conditions[5,7] indicate fractional conversions of SO_2 to SO_3 of the order of a few percent. According to these studies, SO_3 formation occurs primarily through the reaction

$$SO_2 + O\ (+M) \rightarrow SO_3\ (+M) \qquad \text{(R1)}$$

Direct measurements are available for this reaction in the 300−800 K range[8,9] and for the reverse reaction, thermal dissociation of SO_3, in the temperature range of 1700−2500 K.[10] Indirect determinations are available from flames[12−14] and shock tube experiments.[15] The rate constant increases with temperature at lower temperatures, peaks at around 750 K, and drops off as the temperature increases further.[9,10] The positive temperature dependence below 750 K arises from a barrier of about 16 kJ/mol to reaction,[9] while at higher temperatures the dominant effect becomes the limitations in collisional stabilization of the SO_3^* intermediate, causing a decrease in the reaction rate. A Rice−Ramsperger−Kassel−Marcus (RRKM) extrapolation of the low-temperature measurements is in good agreement with data for both the forward and backward reaction over a temperature range of 220−2500 K for Ar as collision partner.[9] Even above 1000 K the reaction is in the falloff region at atmospheric pressure.[7,9]

Reaction 1 is important not only for the formation of SO_3 in combustion systems but also in some industrial processes. In the reverse direction

$$SO_3\ (+M) \rightarrow SO_2 + O\ (+M) \qquad \text{(R1b)}$$

it is believed to be a rate-limiting step in the conversion of spent sulfuric acid to SO_2.[11] Even though the rate constant for reaction R1 is probably known more accurately than most sulfur reactions, it is noteworthy that there are few measurements under the conditions of practical interest in combustion and industrial processes, that is, temperatures between 1000 and 1500 K. Recently, Hwang et al.[15] derived a rate constant for R1 in Ar

† Part of the special issue "David M. Golden Festschrift".

* To whom correspondence should be addressed. E-mail: pgl@KT.DTU.DK.

10.1021/jp0557215 CCC: $33.50
Published on Web 01/12/2006

in the temperature range of 960−1150 K from modeling the effect of SO_2 addition on the OH concentration profile for H_2 oxidation in a shock tube. However, the only direct measurements of the rate constant using nitrogen as collision partner were obtained at room temperature.[8]

The objective of the present work is to derive a rate constant for the thermal dissociation of SO_3 in the 1000−1400 K range from flow reactor experiments with nitrogen as inert gas. A gas containing a mixture of SO_2 and O_2 in N_2 is led to a catalyst, where SO_2 is partly oxidized to SO_3 at 673 K. The resulting gas is then led to a flow reactor, where SO_3 is converted back to SO_2 by thermal dissociation. The fractional conversion of SO_3 in the homogeneous reactor provides a measure of the value of k_{1b}. The results are compared to the RRKM predictions for the $SO_2 + O$ ($+N_2$) reaction. In addition, the more accurate value available for k_1 allows for a reassessment of the rate constant for the reaction $SO_3 + O \rightarrow SO_2 + O_2$ (R2) obtained from flame measurements.[12−14]

Experimental Section

The source of SO_3 in the present study is oxidation of SO_2 over a KCl-doped $V_2O_5-WO_3-TiO_2$ catalyst. Oxidation of SO_2 to SO_3 is a concern in selective catalytic reduction (SCR), a common technology used for the removal of nitrogen oxides in flue gas by reaction with NH_3. Since the presence of SO_3 is detrimental to the ability of vanadium catalysts to remove NO,[16,17] oxidation of SO_2 over commercial catalysts has been the subject of recent research work. Zheng and Jensen[18] studied the kinetics of SO_2 oxidation over SCR catalysts provided by Haldor Topsøe A/S. They tested catalysts with different concentrations of the active component V_2O_5 (<10 wt %) and WO_3 (5−13 wt %). The catalysts were doped with KCl and K_2SO_4 at different levels by a wet impregnation method at room temperature at 0.8 bar absolute pressure followed by drying at 323 K for 15 h. Zheng and Jensen found that, at 673 K, the activity of the doped catalyst for SO_2 oxidation was more than an order of magnitude higher than that of a fresh catalyst and the SO_2 conversion efficiency was fairly constant over time. The catalyst used in this work is the KCl-doped 7.3 wt % $V_2O_5-WO_3-TiO_2$ catalyst from the work of Zheng and Jensen.[18]

The experimental setup consisted of two quartz reactors in series in separate ovens. In the first reactor, SO_2 was oxidized to SO_3 over the doped $V_2O_5-WO_3-TiO_2$ catalyst. The temperature along the catalytic reactor was set to 673 K. The product gas from the first reactor was fed into the second reactor through a heated line at 415 K in order to prevent condensation. The second reactor was homogeneous, operated at high temperatures (up to around 1400 K) to promote the conversion of SO_3 to SO_2.

A schematic of the experimental setup is presented in Figure 1. Sulfur dioxide, oxygen, and nitrogen were mixed in a cross-joint and directed either to bypass (the flow meter, G) or to the catalytic reactor (B). The bubble flow meter served to measure the flow of the input gases from the gas cylinders as a check for mass flow meters. The output of the catalytic reactor was directed either to the homogeneous reactor (C) or to the gas conditioning and analyzers (F). Bypass lines were available for both reactors so that input and output gases could be analyzed and the setup could be used in a flexible way. Prior to the analyzers, a condenser (D) and filters (E) were located to protect the analyzer from any aerosols and/or condensed liquids.

The catalytic reactor was a heterogeneous quartz reactor with a 2 cm inner diameter. The catalyst was cut into pieces (roughly 1.5 cm × 1.5 cm) and stacked upon a porous plate in the isothermal zone of the reactor. The total length of the reactor occupied by the catalyst material was 16 cm. This reactor was operated at 673 K, and the reactor residence time was about 3 s.

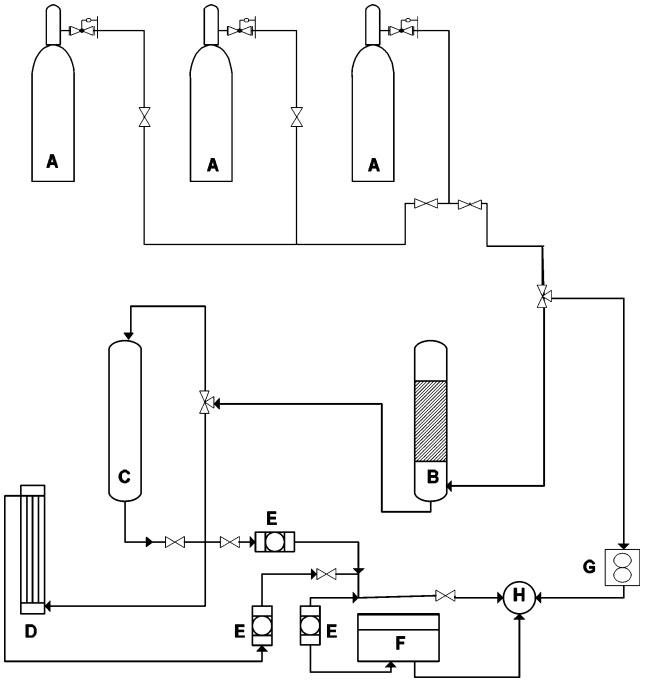

Figure 1. Schematic of the experimental setup: (A) gas cylinders (O_2, SO_2, N_2), (B) catalytic reactor, (C) homogeneous reactor, (D) condenser, (E) filter, (F) gas analyzers, (G) bubble flow meter, and (H) purging system.

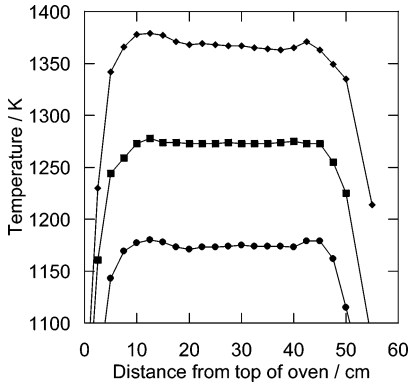

Figure 2. Characteristic temperature profile in the homogeneous reactor.

The homogeneous reactor consisted of a quartz tube located in a three-zone electrically heated oven. No gases were added to the mixture between the first and the second reactor and the reactants entered the homogeneous reactor premixed and were heated together. The tubes used for the second reactor were designed to approximate plug flow in the laminar flow regime.

The reactor temperatures were controlled with thermocouples with an accuracy of ±5 K. During experiments, the thermocouples were placed outside the reactor to avoid contact with the reacting gases but the temperature profiles were obtained from probing inside the reactor with an inert flow. Characteristic temperature profiles for the reactor are shown in Figure 2. In most of the temperature range investigated, a flat temperature profile was obtained in the isothermal region of the reactor, but at the highest temperatures, variations within ±15 K were observed.The concentration of SO_2 was measured continuously by a UV analyzer with an accuracy of ±3%.

TABLE 1: Selected Reactions from the H/S/O Subset[a]

	A	β	E_a/R	ref
1. $SO_2 + O (+N_2) \rightleftharpoons SO_3 (+N_2)$	3.7×10^{11}	0.00	850	9, pw
low-pressure limit	2.9×10^{27}	−3.58	2620	
Troe parameters: 0.43, 371, 7442				
$SO_2 + O (+Ar) \rightleftharpoons SO_3 (+Ar)$	3.7×10^{11}	0.00	850	9
low-pressure limit	2.4×10^{27}	−3.60	2610	
Troe parameters: 0.442, 316, 7442				
2. $SO_3 + O \rightleftharpoons SO_2 + O_2$	7.8×10^{11}	0.00	3070	12, pw
3. $SO_2 + OH \rightleftharpoons SO_3 + H$	4.9×10^{2}	2.69	12000	5
4. $SO_2 + OH (+M) \rightleftharpoons HOSO_2 (+M)$	5.7×10^{12}	−0.27	0	21
low-pressure limit	1.7×10^{27}	−4.09	0	
Troe parameters: 0.10, 1×10^{-30}, 1×10^{30}				
5. $HOSO_2 + O_2 \rightleftharpoons SO_3 + HO_2$	7.8×10^{11}	0.00	330	22

[a] Units are in mol, cm, s, and K.

Numerical Procedure and Reaction Mechanism

The experimental results were interpreted in terms of a detailed reaction mechanism. Since the homogeneous reactor was designed to approximate plug flow, the reactor results were modeled with SENKIN,[19] which is part of the CHEMKIN library.[20] SENKIN performs an integration in time. The results of the SENKIN calculations were compared to experimental data using the nominal residence time in the isothermal part of the reactor.

The reaction mechanism consisted of a H_2/O_2 subset and a full description of the H/S/O reaction system. The H_2/O_2 subset was included in the model to account for effects of water vapor. Presence of water vapor, even in small concentrations, may conceivably lead to an O/H radical pool, initiated by the reaction

$$O + H_2O \rightleftharpoons OH + OH$$

The SO_2/SO_3 subset of the mechanism is listed in Table 1. With a few exceptions, the H/S/O subset and the corresponding thermochemistry were adopted from previous work by the authors.[4,6] The rate coefficients for $SO_2 + O (+N_2) = SO_3 (+N_2)$ (R1b) were estimated from RRKM calculations as part of this study (described below) and used in the modeling. In addition to thermal dissociation of SO_3 (R1b), reactions that consume SO_3 include $SO_3 + O$ (R2), $SO_3 + H$ (R3b), and $SO_3 + HO_2$ (R4b). Also, the oxidation of SO_2 to SO_3 must be taken into consideration; this may occur through the reaction of SO_2 with O (R1) or with OH, either directly (R3) or through $HOSO_2$ (R4, R5).

The reaction $SO_3 + O = SO_2 + O_2$ (R2), an important consumption step for SO_3 under the present conditions, has not been measured directly, and the rate constant is associated with a considerable uncertainty.[5,6] To obtain a reliable estimate of R2 in the temperature range of the present work, we reinterpreted the flame data of Smith et al.[12] They conducted experiments on a low-pressure $CO/O_2/Ar$ flame doped with SO_2. On the basis of measured profiles of SO_2, SO_3, O_2, and O, Smith et al. were able to derive rate constants for reactions $R1_{Ar}$ and R2 in the temperature range of 1435−1850 K. We take a different approach and look at the lower temperature part of the flame closer to the burner surface. In this part, $[SO_3]$ builds up and peaks at a location corresponding to a temperature of 1269 K. At this point in the flame, the net SO_3 formation rate $\dot{R}_{SO_3} = 0$. A reaction analysis shows that SO_3 is formed by reaction $R1_{Ar}$ and consumed almost solely by reaction R2; the temperature is too low for reaction R2b to contribute significantly to the decomposition of SO_3. At this location

$$\dot{R}_{SO_3} = k_{1,Ar}[SO_2][O][M] - k_2[SO_3][O] = 0 \qquad (1)$$

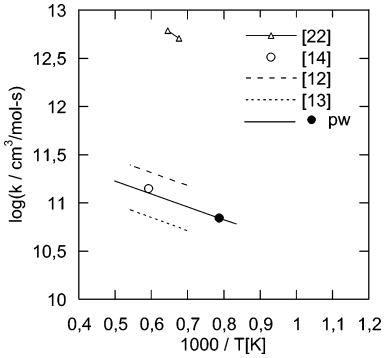

Figure 3. Arrhenius plot for the reaction $SO_3 + O \rightarrow SO_2 + O_2$ (R2). The data shown are obtained in the present work (pw) and from flame measurements: Schofield,[23] Merriman and Levy,[14] and Smith et al.[12,13]

The value of k_2 is then easily derived

$$k_2 = \frac{k_{1,Ar}[SO_2][O][M]}{[SO_3][O]} = \frac{k_{1,Ar}[SO_2][M]}{[SO_3]} \qquad (2)$$

Since the concentration of the O atom drops out of the equation, the uncertainty in the value of k_2 is associated with uncertainties in $k_{1,Ar}$ (adopted from Naidoo et al.[9]) and the measurements of $[SO_2]$, $[SO_3]$, and flame temperature. We obtain a value of k_2 (1269 K) = 6.9×10^{10} cm^3 mol^{-1} s^{-1} with an estimated uncertainty of less than a factor 3. The rate coefficient for R2 is then estimated by adopting the activation energy of 25.5 kJ/mol for the reaction determined by Smith et al.[12] (see Table 1), yielding a rate constant of $k_2 = 7.8 \times 10^{11} \exp(-3065/T)$ cm^3 mol^{-1} s^{-1}. This expression is in excellent agreement with the results of Merryman and Levy[14] who obtained a value of $k_2 = 1.5 \times 10^{11}$ cm^3 mol^{-1} s^{-1} at 1685 K in an atmospheric-pressure flame. A reevaluation of their data with a revised value of $k_{1,Ar}$[9] yields only a small correction in this value (k_2 (1685 K) = 1.4×10^{11} cm^3 mol^{-1} s^{-1}).

Our preferred rate constant for R2 is compared with values reported from flame studies in Figure 3. Apart from the high value recommended by Schofield[23] from a review of early flame measurements, the data are in good agreement. Data from reactor studies of the reaction in the same temperature range (not shown) span more than 5 orders of magnitude and are clearly outside the uncertainty limits of the present recommendation. The flow reactor work of Burdett et al.[24] on the reverse reaction $SO_2 + O_2 = SO_3 + O$ (R2b) in the 900−1350 K range must be in error, since their derived value of k_{2b} corresponds to $k_2 \approx 10^{17}$ cm^3 mol^{-1} s^{-1} at 1000 K, that is, much larger than collision frequency. On the other hand, the value proposed by Alzueta et al.[6] from the analysis of batch reactor data[25] at 1173−1323 K is 2 orders of magnitude lower than the rate constants derived from flames. Such a low value is incompatible with the flame results as well as with the present experimental results; this is discussed further below. Our current thinking is that the batch reactor data may have been influenced by surface loss of SO_3.

Results and Discussion

The experiments were performed at atmospheric pressure with temperatures in the homogeneous reactor in the range 973−1423 K. Typical conditions involved SO_3 and SO_2 concentrations into the homogeneous reactor of about 500 ppm, with around 5% O_2 in N_2. Also, trace amounts of water vapor were present, estimated to be in the range of 30−150 ppm.[26] A typical experimental run is shown in Figure 4. At $t = 0$, only the nitrogen and oxygen valves were turned on and the two reactors

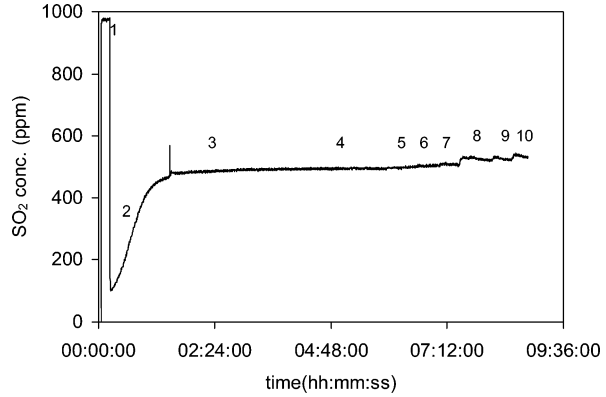

Figure 4. Characteristic SO_2 profile as a function of time in an experiment. The inlet gas contains 975 ppm SO_2 and 4.7 O_2, with trace amounts of water vapor and N_2 as the carrier gas: (1) The input concentration of SO_2 is analyzed. (2) The gas is fed to the catalytic reactor, bypassing the homogeneous reactor. The products from the catalytic reactor are analyzed. (3) After the catalytic reactor has achieved steady-state operation, the product gas from this reactor is fed into the homogeneous reactor (operated at 923 K). The product gas from the homogeneous reactor is analyzed. (4−10) Step 3 is repeated for temperatures of 948, 973, 998, 1023, 1048, 1073, and 1176 K.

were bypassed. Then, SO_2 was supplied to the system, and the inlet SO_2 concentration was measured. The reactant gas mixture was then fed into the catalytic reactor, resulting in a rapid oxidation of SO_2. The initial conversion was more than 80%, but over time the conversion efficiency decreased, and in about 45 min, the SO_2 concentration stabilized at about 500 ppm. The conversion efficiency of the catalytic reactor depended on the SO_2/O_2 ratio; a 35−60% conversion of SO_2 to SO_3 was observed for SO_2/O_2 ratios between 0.01 and 0.1. Once the SO_2 concentration out of the catalytic reactor was stabilized, the product gas was fed into the homogeneous reactor. The temperature in the homogeneous reactor was increased in steps of 25 K above the chosen starting temperature, securing steady-state conditions between each temperature increment. As indicated by the results of Figure 4, thermal dissociation of SO_3 was very slow below 1100 K and subsequent experiments emphasized temperatures above this value.

Experimental results for the decomposition of SO_3 in the temperature range of 1050−1425 K are shown in Figure 5. The five experimental runs cover sulfur oxide levels in the range of 580−1050 ppm and oxygen concentrations of 2.6−5.0%. Over this temperature range, the SO_3 conversion increased from being negligible to being almost complete. The oxygen level affects the oxidation of SO_2 to SO_3 in the catalytic reactor but has little effect on the SO_3 decomposition in the homogeneous reactor.

Figure 6 compares selected experimental data (sets 1 and 4) to modeling predictions with the detailed reaction mechanism (solid lines). Without any adjustments, the kinetic model is seen to describe the experimental results quite well. For all sets, the kinetic model is in agreement with the experimental data within experimental uncertainty.

Sensitivity analysis of the calculations with the detailed chemical kinetic model shows that the SO_3 decomposition rate is only sensitive to two reactions

$$SO_3\,(+M) \rightleftharpoons SO_2 + O\,(+M) \qquad \text{(R1b)}$$

$$SO_3 + O \rightleftharpoons SO_2 + O_2 \qquad \text{(R2)}$$

The chemistry is not affected by the trace impurities of water vapor present.

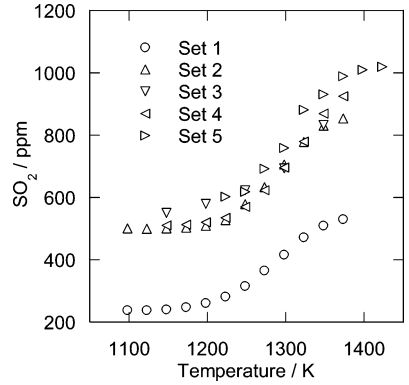

Figure 5. Experimental results for thermal decomposition of SO_3. Set 1: $SO_3 = 342$ ppm, $SO_2 = 238$ ppm, $O_2 = 4.7\%$; residence time $2320/T$(K). Set 2: $SO_3 = 420$ ppm, $SO_2 = 500$ ppm, $O_2 = 2.6\%$; residence time $2550/T$(K). Set 3: $SO_3 = 406$ ppm, $SO_2 = 540$ ppm, $O_2 = 4.7\%$; residence time $2901/T$(K). Set 4: $SO_3 = 487$ ppm, $SO_2 = 510$ ppm, $O_2 = 4.7\%$; residence time $2164/T$(K). Set 5: $SO_3 = 467$ ppm, $SO_2 = 578$ ppm, $O_2 = 5.0\%$; residence time $1873/T$(K). All experiments are carried out with N_2 as the carrier gas, with $H_2O \approx 100$ ppm, and with a pressure of about 1.05 atm. The residence time (s), varying with reactor temperature as indicated (constant mass flow), applies to the isothermal part of the reactor (about 40 cm of the length).

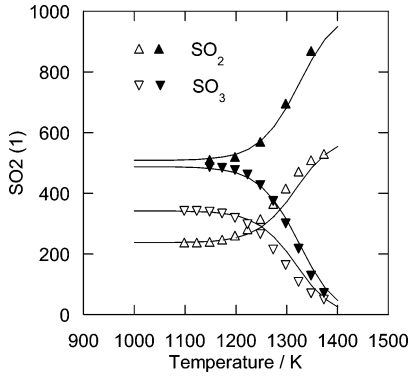

Figure 6. Comparison between experimental results (symbols) and modeling predictions (solid lines) for thermal decomposition of SO_3. Set 1 (open symbols): $SO_3 = 342$ ppm, $SO_2 = 238$ ppm, $O_2 = 4.7\%$; residence time $2320/T$(K). Set 4 (closed symbols): $SO_3 = 487$ ppm, $SO_2 = 510$ ppm, $O_2 = 4.7\%$; residence time $2164/T$(K). The outlet SO_3 concentration is calculated as the difference between the inlet and outlet SO_2. The experiments are carried out with N_2 as the carrier gas, with $H_2O \approx 100$ ppm, and with a pressure of about 1.05 atm.

The rate constant of reaction R1b was determined from optimization of the value of k_{1b} at selected experimental conditions using the detailed chemical kinetic model. Figure 7 summarizes the values of k_{1b} obtained from the experimental runs. We have disregarded data obtained at low (<20%) or high (>80%) conversions of SO_3. There is some scatter in the data, but within the uncertainty, values appear to be independent of the SO_x inlet level and the O_2 concentration, as would be expected. The flow reactor data are consistent with a rate constant for $SO_3 + N_2 \rightleftharpoons SO_2 + O + N_2$ of 5.7×10^{17} exp$(-40000/T)$ cm^3/(mol s) in the temperature range of 1273−1348 K.

Similar, but slightly lower, values of k_{1b} could be obtained from a simple analysis of the R1b−R2 reaction sequence, assuming the oxygen atom is in the steady state. Reaction R2 can be assumed to be irreversible, since the reverse step, $SO_2 + O_2$, is endothermic by about 150 kJ/mol. The decomposition rate for SO_3 can be written as

$$\dot{R}_{SO_3} = -k_{1b}[SO_3][M] - k_2[SO_3][O] + k_1[SO_2][M] \quad (3)$$

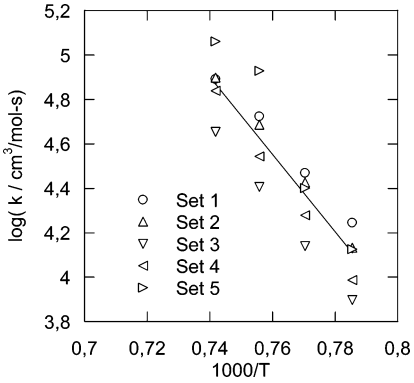

Figure 7. Values of the rate constant for $SO_3 + N_2$ (R1b) determined from the results of the flow reactor experiments. The solid line is a best-fit line to the data, corresponding to $k_{1b} = 5.7 \times 10^{17} \exp(-40000/T)$ cm^3/(mol s). The values were obtained from data at fractional conversions of SO_3 between 20 and 80%.

The steady-state concentration of O is then

$$[O]_{ss} = \frac{k_{1b}[SO_3][M]}{k_1[SO_2][M] + k_2[SO_3]} \quad (4)$$

Inserting the expression for $[O]_{ss}$, we get after some manipulation

$$\dot{R}_{SO_3} = k_{1b}[SO_3][M]\left[\frac{k_1[SO_2][M] - k_2[SO_3]}{k_1[SO_2][M] + k_2[SO_3]} - 1\right] \quad (5)$$

An assumption that $k_2[SO_3] \gg k_1[SO_2][M]$ leads to a simple expression for the SO_3 consumption rate, $-\dot{R}_{SO_3} = 2k_{1b}[SO_3][M]$, from which k_{1b} can easily be obtained. Since R2 is comparatively fast according to the flame measurements, the inequality is almost fulfilled and the error in the values in k_{1b} from the simple analysis, compared to the detailed analysis, is only of the order of 30%. It is noteworthy that a very low value for k_2, such as that proposed by Alzueta et al.,[6] leads to $k_1[SO_2][M] \gg k_2[SO_3]$ and thereby $\dot{R}_{SO_3} = 0$. This is in conflict with the experimental observations; the present flow reactor data support the comparatively high value for k_2 derived from flames.

The error analysis conducted includes an experimental uncertainty and a modeling uncertainty. The experimental uncertainty involves uncertainty in inlet concentrations, outlet concentrations, reactor residence time in the isothermal zone, reactor temperature, and the potential loss of SO_3 or O atoms on the reactor surface; the modeling uncertainty involves uncertainty in the value of k_2. Of special concern, is the potential impact of reactions on the surface of the quartz reactor. Sulfur trioxide is known to absorb on glass surfaces where it may act to promote the recombination of atomic oxygen.[27,28] However, an experiment conducted in a flow reactor with half the diameter (i.e., twice the surface-to-volume ratio) of the standard reactor yielded a value of k_{1b}, which within the scatter was in agreement with the data from the larger reactor. From an assessment of each contribution, we estimate the overall uncertainty in k_{1b} to be a factor of 2.

Figure 8 compares the data for the thermal dissociation rate of SO_3 with the only other measurements of this reaction, the shock tube study of Astholz et al.[10] While the present study involved nitrogen as collision partner, Astholz et al. conducted their experiments in argon. The two sets of data appear to be consistent, but a direct comparison is difficult due to the differences in the temperature regime and bath gas.

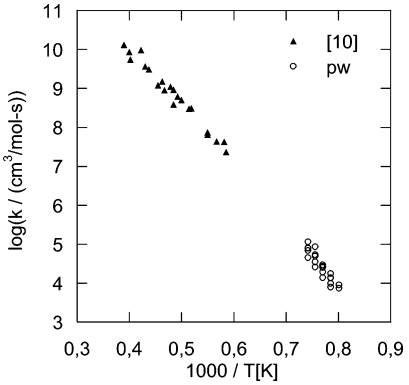

Figure 8. Arrhenius plot for the reaction $SO_3 + M \rightarrow SO_2 + O + M$ (R1b). The open symbols denote values obtained in the present work (pw), while the closed symbols represent the measurements of Astholz et al.[10] with Ar as the third body.

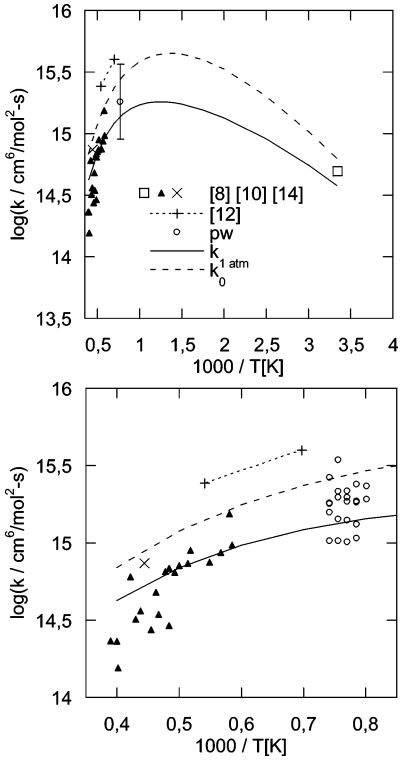

Figure 9. Arrhenius plot for the reaction $SO_2 + O + M \rightarrow SO_3 + M$ (R1). The upper part shows results for the 300−2500 K temperature range, while the lower part emphasizes the high-temperature results. The lines represent RRKM calculations originally adjusted to fit measurements for M = Ar but rescaled for N_2. The solid lines are the rate constant at 1 atm, while the dashed lines represent the low-pressure limit. The data shown are from the present work (pw) and from the literature: Atkinson and Pitts, Jr.,[8] Merriman and Levy,[14] Astholz et al.,[10] and Smith et al.[12] All data refer to the $SO_2 + O + N_2$ reaction, except the measurements of Astholz et al.[10] and Smith et al.,[12] which were performed with Ar as the third body.

In Figure 9, the results are compared with the theoretical rate constant for the reverse reaction, $SO_2 + O + N_2 \rightarrow SO_3 + N_2$ (R1), as well as selected literature results. The latter include the room-temperature result of Atkinson and Pitts, Jr.[8] and indirect measurements by Merryman and Levy from flames.[14] The results from the flow reactor study of Mueller et al.[7] and the shock tube study of Hwang et al.[15] on the reaction are not included, since they were obtained at higher pressures. The high-temperature data of Astholz et al.[10] and Smith et al.[12] are shown, even though they relate to argon as a bath gas. The values of k_1

from the present work and from Astholz et al. were derived from k_{1b} through the equilibrium constant for the reaction.

The upper part of Figure 9 shows results over a broad range of temperature, while the lower part emphasizes the high-temperature results. The solid and dashed lines in Figure 9 denote the theoretical rate constant for $SO_2 + O$ ($+N_2$) at 1 atm and at the low-pressure limit, respectively. The high-pressure limit was taken from Naidoo et al.[9] Troe's unimolecular formalism has previously been applied to R1 with M = Ar, to obtain the broadening parameter F_c and, by fitting to measurements over 290−840 K, the average energy transfer per collision $-\langle\Delta E\rangle = 3000\ \mathrm{J}(T/298)^{-0.42}$.[9] That representation of the falloff curves was reevaluated in this study for M = N_2. Collision rates with the bath gas were calculated in the same way as outlined earlier[9] based on $\sigma = 3.62$ and $\epsilon/k = 97.5$ K for N_2. To match the ratio $k_{1,0}(N_2)/k_{1,0}(Ar) = 1.3$ determined by Atkinson and Pitts at room temperature,[8] we chose $-\langle\Delta E\rangle = 5740$ J for N_2 collisions and assumed the same temperature dependence as for Ar. The new broadening parameter is given in Table 1, along with the $k_{1,0}$ expression for M = N_2. This expression fits the Troe formulation to within about 15%. Comparison with the expression for M = Ar[9] indicates similar rate constants at the low-pressure limit, with $k_{1,0}(N_2)/k_{1,0}(Ar) \approx 1.2$ and little temperature dependence of this ratio.

The results in Figure 9 confirm that the recombination of sulfur dioxide with oxygen atoms has a positive activation energy at low temperatures, while at high temperatures the reaction rate decreases with temperature. The reaction appears to be in the falloff region at atmospheric pressure over a wide range of temperature, including the conditions of the present work. The value of k_1 derived from the flow reactor data is seen to be in good agreement with the theoretical rate coefficients. According to the present study, the rate constant using N_2 as collision partner does not deviate much from that using Ar. It is worthwhile to compare the present results with those of Mueller et al.,[7] who studied the high-pressure falloff behavior of the reaction. Under the conditions of the present work (1000−1400 K, atmospheric pressure), their proposed rate constant for $SO_2 + O$ ($+N_2$) is in very good agreement with the present work, being within 25% of our theoretical value. Within the uncertainty, the present results are also in agreement with the shock tube results of Hwang et al.;[15] they derived a value of k_1 of $(3.9 \pm 2.0) \times 10^{15}$ cm^6 mol^{-2} s^{-1} at 960−1150 K and pressures of 1.3−2.7 atm.

Concluding Remarks

On the basis of experiments conducted in a laminar flow reactor, a rate constant for $SO_3 + N_2 \rightarrow SO_2 + O + N_2$ (R1b) of $5.7(^{+5.7}_{-2.9}) \times 10^{17}$ exp(−40000/T) cm^3/(mol s) was derived for the temperature range of 1273−1348 K and atmospheric pressure. The temperature and pressure dependence of the reverse reaction, $SO_2 + O$ ($+N_2$), were estimated based on RRKM calculations for $SO_2 + O$ ($+$Ar),[9] rescaling for N_2. The theoretical rate coefficients agree with the experimental value within the uncertainty. On the basis of the flame measurements of Smith et al.[12] and the present value of $k_{1,Ar}$, the rate constant for $SO_3 + O \rightarrow SO_2 + O_2$ (R2) was estimated to be 6.9×10^{10} cm^3 mol^{-1} s^{-1} at 1269 K, with an uncertainty factor of 3. The recommended rate constant $k_2 = 7.8 \times 10^{11}$ exp(−3065/T) cm^3 mol^{-1} s^{-1} is consistent with other flame results as well as the present flow reactor data.

Acknowledgment. The authors acknowledge support from the CHEC (Combustion and Harmful Emission Control) Research Program, PSO-Elkraft (Grant FU-2207), the National Science Foundation (Grant CTS-0113605), the Robert A. Welch Foundation (Grant B-1174), and the UNT Faculty Research Fund.

References and Notes

(1) Johnsson, J. E.; Glarborg, P. Sulfur Chemistry in Combustion I - Sulfur in Fuels and Combustion Chemistry. *Pollutants from Combustion. Formation Mechanisms and Impact on Atmospheric Chemistry*; Vovelle, C., Ed.; Kluwer Academic Publisher: Boston, MA, 2000; pp 283−301.

(2) Christensen, K. A.; Livbjerg, H. *Aerosol Sci. Technol*. **1996**, *25*, 185−199.

(3) Jensen, J. R.; Nielsen, L. B.; Schultz-Møller, C.; Wedel, S.; Livbjerg, H.; *Aerosol Sci. Technol*. **2000**, *33*, 490−509.

(4) Glarborg, P.; Marshall, P. *Combust. Flame* **2005**, *141*, 22−38.

(5) Glarborg, P.; Kubel, D.; Dam-Johansen, K.; Chiang, H. M.; Bozzelli, J. W. *Int. J. Chem. Kinet*. **1996**, *28*, 773−790.

(6) Alzueta, M. U.; Bilbao, R.; Glarborg, P. *Combust. Flame* **2001**, *127*, 2234−2251.

(7) Mueller, M. A.; Yetter, R. A.; Dryer, F. L. *Int. J. Chem. Kinet*. **2000**, *32*, 317−339.

(8) Atkinson, R.; Pitts, J. N., Jr. *Int. J. Chem. Kinet*. **1978**, *10*, 1081−1090.

(9) Naidoo, J.; Goumri, A.; Marshall, P. *Proc. Combust. Inst.* **2005**, *30*, 1219−1225.

(10) Astholz, D. C.; Glänzer, K.; Troe, J. *J. Chem. Phys.* **1979**, *70*, 2409−2413.

(11) Schwartz, D.; Gadiou, R.; Brilhac, J. F.; Prado, G.; Martinez, G. *Ind. Eng. Chem. Res.* 2000, 39, 2183-2189.

(12) Smith, O. I. Tseregounis, S.; Wang, S.-N. *Int. J. Chem. Kinet*. **1982**, *14*, 679−697.

(13) Smith, O. I. Tseregounis, S.; Wang, S.-N.; Westbrook, C. K. *Combust. Sci. Technol*. **1983**, *30*, 241−271.

(14) Merryman, E. L.; Levy, A. *Proc. Combust. Inst.* **1979**, *17*, 727−736.

(15) Hwang, S. M.; Cooke, J. A.; DeWitt, K. J.; Rabinowitz, M. J. Determination of Rate Coefficients of $SO_2 + O + M \rightarrow SO_3 + M$ Reaction. 30th International Symposium on Combustion, Work-In−Progress poster, Chicago, IL, July 25−30, 2004.

(16) Dunna, J. P.; Stenger, H. G., Jr.; Wachs, I. E. *Catal. Today* **1999**, *51*, 301−318.

(17) Giakoumelou, I. Parvulescu, V.; Boghosian, S. *J. Catal*. **2004**, *225*, 337−349.

(18) Zheng, J.; Jensen, A. D. Unpublished results.

(19) Lutz, A.; Kee, R. J.; Miller, J. A. *SENKIN: A Fortran Program for Predicting Homogeneous Gas-Phase Chemical Kinetics with Sensitivity Analysis*; Sandia Report SAND87-8248; Sandia National Laboratories: Livermore, CA, 1987.

(20) Kee, R. J.; Rupley, F. M.; Miller, J. A. *CHEMKIN-II: A Fortran Chemical Kinetics Package for the Analysis of Gas-Phase Chemical Kinetics*; Sandia Report SAND89-8009; Sandia National Laboratories: Livermore, CA, 1989.

(21) Blitz, M. A.; Hughes, K. J.; Pilling, M. J. *J. Phys. Chem. A* **2003**, *107*, 1971−1978.

(22) Atkinson, R.; Baulch, D. L.; Cox, R. A.; Hampson, R. F.; Kerr, J. A.; Troe, J. *J. Phys. Chem. Ref. Data* **1992**, *21*, 1125−1568.

(23) Schofield, K. *J. Phys. Chem. Ref. Data* **1973**, *2*, 25−84.

(24) Burdett, N. A.; Langdon, W. E.; Squires, R. T. *J. Inst. Energy* **1984**, 373.

(25) Cullis, C. F.; Henson, R. M.; Trimm, D. L. *Proc. R. Soc. London, Ser. A* **1966**, *295*, 72−83.

(26) Kristensen, P. G. Nitrogen Burnout Chemistry. Ph.D. Thesis, Department of Chemical Engineering, Technical University of Denmark, Lyngby, Denmark, 1997.

(27) Kaufman, F. *Proc. R. Soc. London, Ser. A* **1958**, *247*, 123−139.

(28) Cullis, C. F.; Mulcahy, M. F. R. *Combust. Flame* **1972**, *18*, 225−292.